PhotoElectroChemistry for Corrosion

M. Skocic, PhD Electrochemistry and Materials

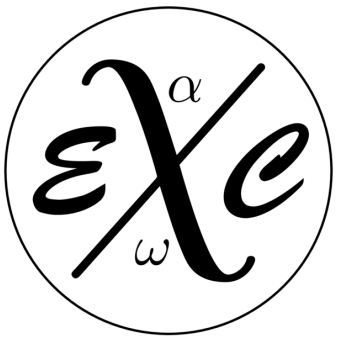

Contents

Introduction

Photoelectrochemical techniques have been shown to be useful tools for characterizing oxidation layers.

Interdisciplinary theoretical underpinnings were built [1–5] such as the Gärtner-Butler model [6, 7] which has been proven to be a simple and robust model for the photocurrent generation.

Technical progresses were achieved, allowing to study oxide layers at macroscopic, mesoscopic, and microscopic scales [8, 9], or in-situ in high temperature corrosion conditions [10, 11].

Hypotheses

Several hypotheses are needed in order to apply the theoretical concepts:

- semiconductors are considered to be ideal i.e. crystallized and homogeneous
- the dielectric constant of the semiconductor is independent of the light wavelength
- the capacity of the Helmholtz layer is greater than the capacitance of the space charge capacitance
- the potential drop in the Helmholtz layer is independent of the applied potential and is negligible

Warning

The hypotheses are rarely fully respected in the case of oxides or passive films formed on industrial alloys. Nonetheless, the literature shows that the developed models can be applied to non-ideal systems such as oxides and passive films.

Band Model I

Solids: conductors, semiconductors and insulators.

Valence and conduction bands correspond to allowed energy states for the electrons.

E_c is the lowest energy level of the conduction band.

E_v is the highest energy level of the valence band.

E_g is the band gap with no allowed energy states.

E_F is the Fermi Level which describes the distribution of the electrons among both bands. It represents the highest energy state that can be occupied level at 0K. It is equivalent to the electrochemical potential in solid phases.

Band Model II

The electronic conduction = movement of electrons and/or holes in conduction/valence band.

The conduction depends on the number of available charge carriers in the conduction band and in the valence band.

In conductors: overlap of the conduction and the valence bands occurs.

In semiconductor and insulator: the conduction depends on the band gap and the energy provided by the environment to the electrons from the valence band in order to jump into the conduction band.

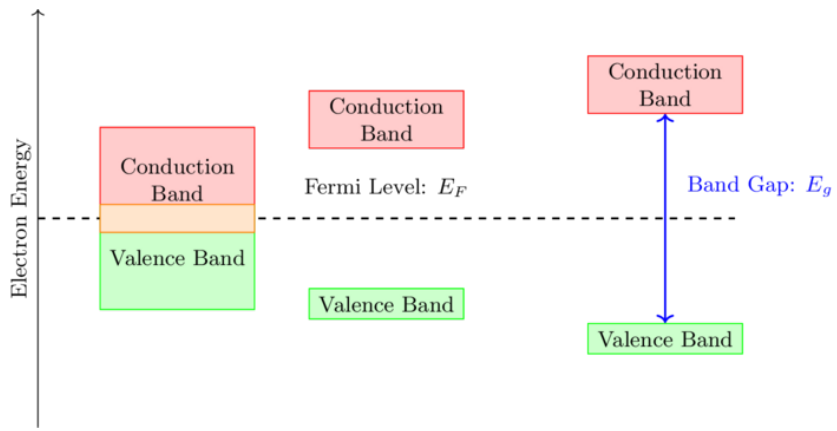

Excitation carrier

In semiconductors, charge carriers can be generated by three mechanisms:

- thermal excitation: in the case of very low band gaps, it can be enough in order to eject an electron from E_v to E_c.
- photoexcitation: ejects electrons from E_v to E_c band when an incident photon ($h\nu > 5eV$) is absorbed.
- doping: introduces additional energy level located in between E_v to E_c.

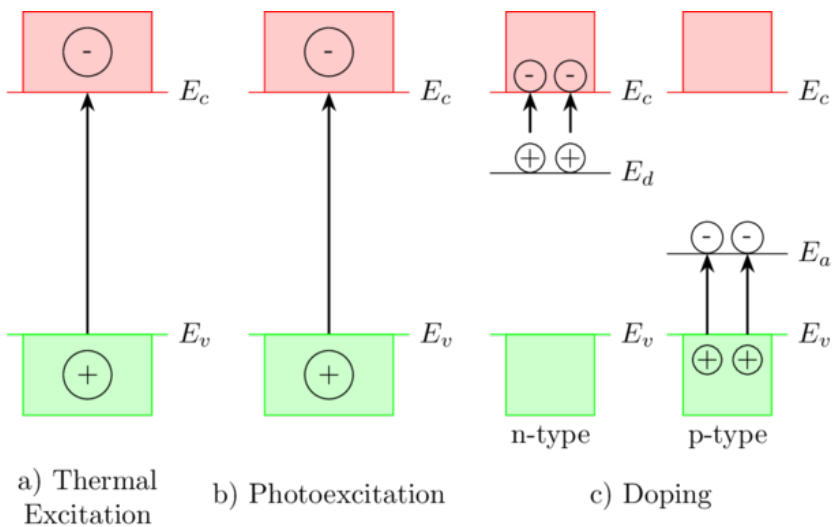

Fermi Level Position

The Fermi level E_F in intrinsic semiconductors is located at the mid-gap.

The n-type and p-type doping shift the Fermi level towards band edges E_c and E_v.

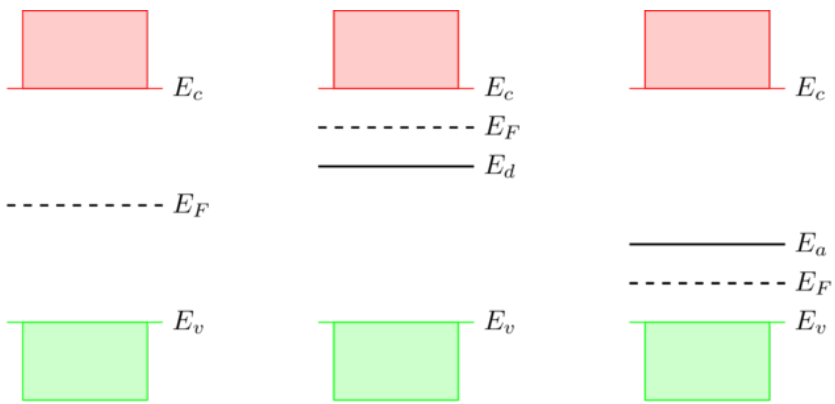

a) Intrinsic b) n-type b) p-type

Band Bending I

A potential gradient occurs when a semiconductor comes into contact with an electrolyte.

Φ_{sc} and Φ_{el} correspond to the potentials of the semiconductor and the electrolyte, respectively.

$\Delta Phi_{sc/el}$ corresponds to the potential difference between the semiconductor and the electrolyte.

w_{sc} and w_H correspond to the widths of the space charge and the electrical double layer, respectively.

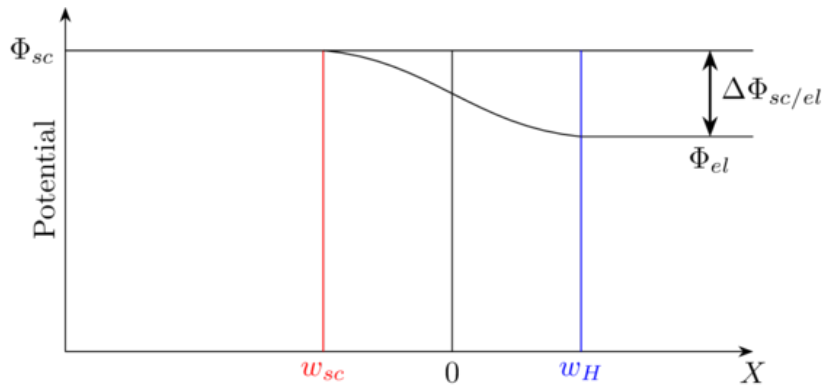

Band Bending II

The position of the Fermi level in the electrolyte with respect to the conduction and valence band edges leads to three different situations after a transient charge transfer:

- flat band
- depletion
- accumulation

The flat band situation occurs when the Fermi level in the electrolyte matches the Fermi level in the semiconductor.

Consequently, there is no potential gradient in the semiconductor.

In a case of Fermi level mismatch, a band bending occurs in the semiconductor near the semiconductor/electrolyte interface.

Band Bending III

The band bending leads to either depletion or accumulation of majority charge carriers near the semiconductor/electrolyte interface.

The spatial extension of the depletion/accumulation zone is called space charge.

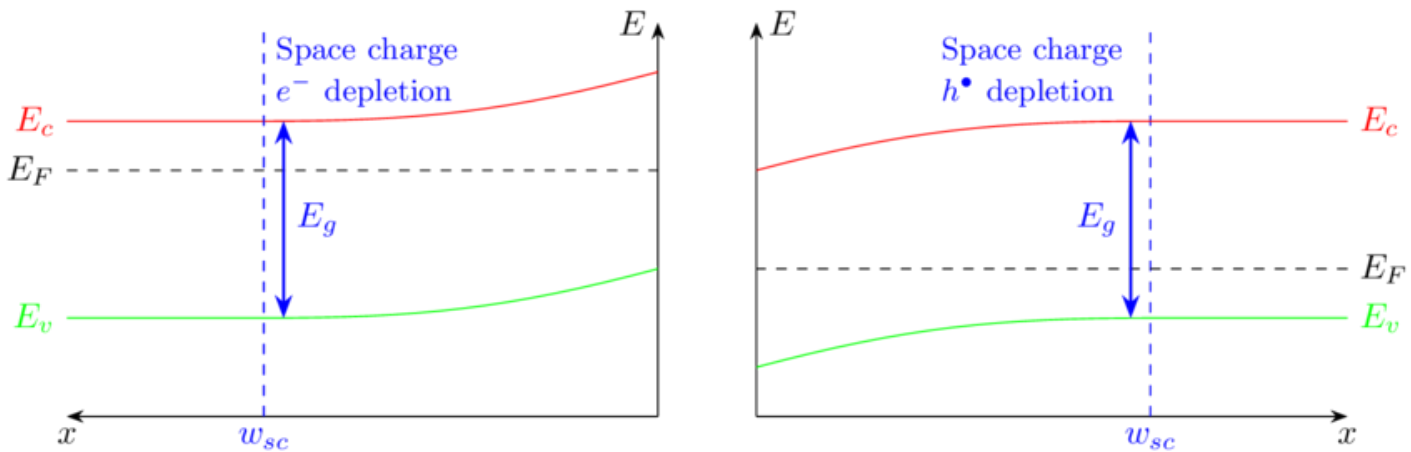

a) n-type b) p-type

Electron/hole pairs I

The illumination of the semiconductor/electrolyte interface, with photons having an energy greater than the band gap, E_g, creates electron/hole pairs in the semiconductor.

By applying the adequate potential the pairs can be separated.

As a consequence, the majority charge carriers are attracted to the semiconductor bulk whereas the minority charge carriers are drawn to the semiconductor/electrolyte interface where they can be transferred to a RedOx species creating an additional current called photocurrent.

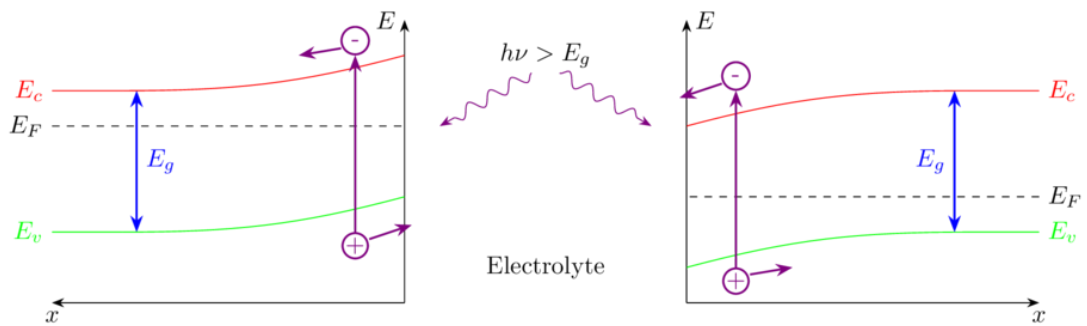

a) n-type b) p-type

Electron/hole pairs II

The photocurrent is significant when the semiconductor/electrolyte junction is in depletion.

n-type (p-type) semiconductors generate anodic (cathodic) photocurrents where the electrons (holes) move towards the external circuit whereas the holes (electrons) move towards the interface.

The applied potential on n-type (p-type) semiconductors is greater (lower) than the flat band potential.

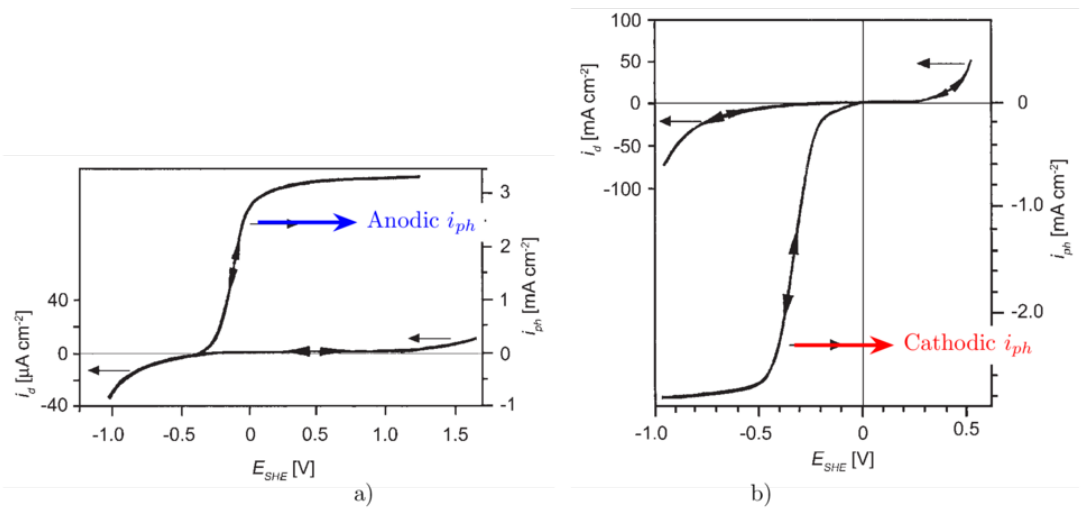

Gärtner-Butler Model I

Gärtner [6] and Butler [7] proposed a simple and robust model for describing the photocurrent.

The photocurrent depends on:

- w_{sc}: space charge width
- α: absorption coefficient
- L_{cc}: the average diffusion length of the minority charge carriers

$$I_{ph} = \phi_0 \left[1 - \frac{\exp(-\alpha_{sc} \cdot w_{sc})}{1 + \alpha_{sc} \cdot L_{cc}} \right] \tag{1}$$

When $\alpha_{sc} \cdot w_{sc} \ll 1$ and $\alpha \cdot L_{cc} \ll 1$, the photocurrent is approximated by the equation 2.

$$I_{ph} = \phi_0 \cdot \alpha \cdot w_{sc} \tag{2}$$

Gärtner-Butler Model II

Space charge width w_{sc} in depletion depends on:

- N_{cc}: number of majority charge carriers ($\sim$ doping)
- e: elementary charge of an electron
- U, U_{fb}: applied, flat band potentials
- ϵ, ϵ_0: relative, vacuum permittivity

$$w_{sc} = \sqrt{\frac{2\epsilon\epsilon_0}{eN_{cc}}(U - U_{fb} - \frac{kT}{e})} \tag{3}$$

The absorption coefficient α_{sc} depends on $h\nu$ (light energy) and n (band-band transition type).

$$\alpha_{sc} = const\frac{(h\nu - E_g)^n}{h\nu} \tag{4}$$

Gärtner-Butler Model III

The photocurrent is therefore given by the equation 5.

$$I_{ph} = \phi_0 \cdot const \frac{(h\nu - E_g)^n}{h\nu} \cdot \sqrt{\frac{2\epsilon\epsilon_0}{eN_{cc}}(U - U_{fb} - \frac{kT}{e})} \tag{5}$$

The linear transform with respect to the energy is used for determining the band gaps.

$$\left[\frac{I_{ph} \cdot h\nu}{\phi_0}\right]^{1/n} = const \cdot (h\nu - E_g) \tag{6}$$

The linear transform with respect to the potential is used for determining the semiconducting type, the flat band potential, and the number of majority charge carrier.

$$I_{ph}^2 = const \cdot (U - U_{fb} - \frac{kT}{e}) \tag{7}$$

Identification of minor oxides

Benaboud et al. [8] showed that the photoelectrochemical characterization is robust for detecting the presence of minor oxides.

The strong photocurrent observed at around 5 eV reveals the major oxide i.e. monoclinic zirconia. The photocurrent $h\nu < 5eV$ reveals the presence of minor oxides even in "pure" zirconium.

The slope changes provided an estimation of the band gaps: hematite, chromia and a solid solution of $(Fe_x Cr_{1-x})O_3$.

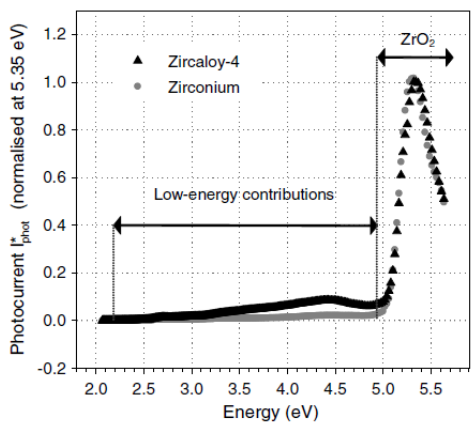

(a)

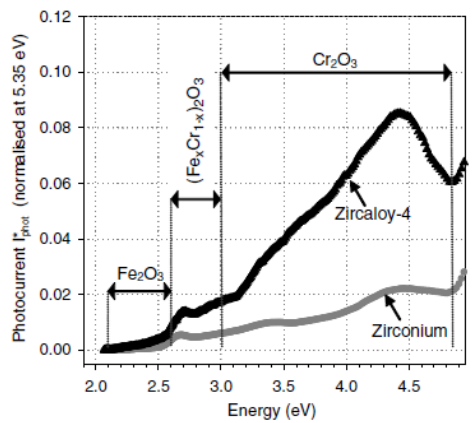

(b)

Semiconduction type

Loucif et al. [12] showed the effect of hydrogen pressure on the semiconduction type on Ni-based alloy 600 oxidized in simulated PWR.

The "V-shape" of the normalized photocurrent reveals an isolating behavior of the oxide layer at high hydrogen pressure.

The monotonous increase of the normalized photocurrent towards more anodic potentials reveals n-type semiconduction.

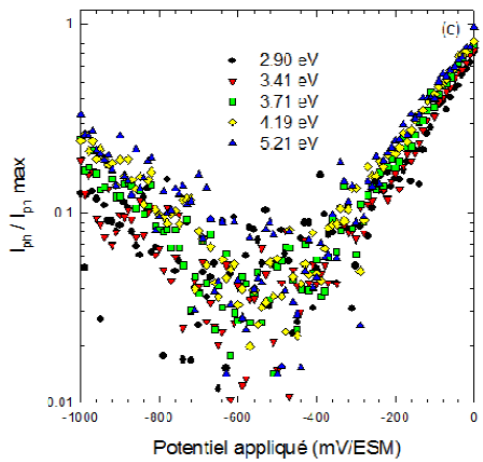

(a)

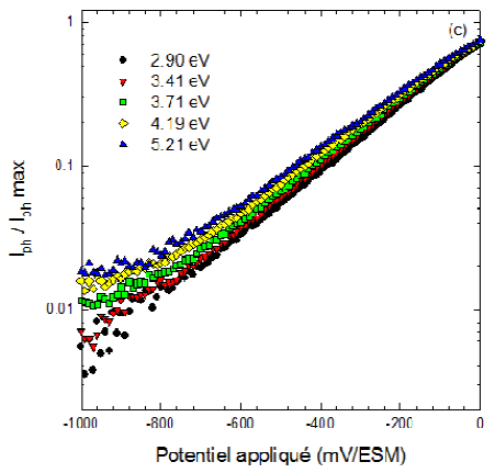

(b)

High temperature PEC I

The majority of photoelectrochemical characterizations are performed at room temperature in simple glass/Plexiglas cells where the signal/noise ratio is very good.

High temperature photoelectrochemical characterizations require sophisticated metallic cells and transparent windows able to withstand the arch environment.

Despite the need to improve the signal/noise ratio, the feasibility of the in-situ photoelectrochemical characterizations was demonstrated by Bojinov et al. [10] in 2002 and more recently by Skocic [11] in 2015

High temperature PEC II

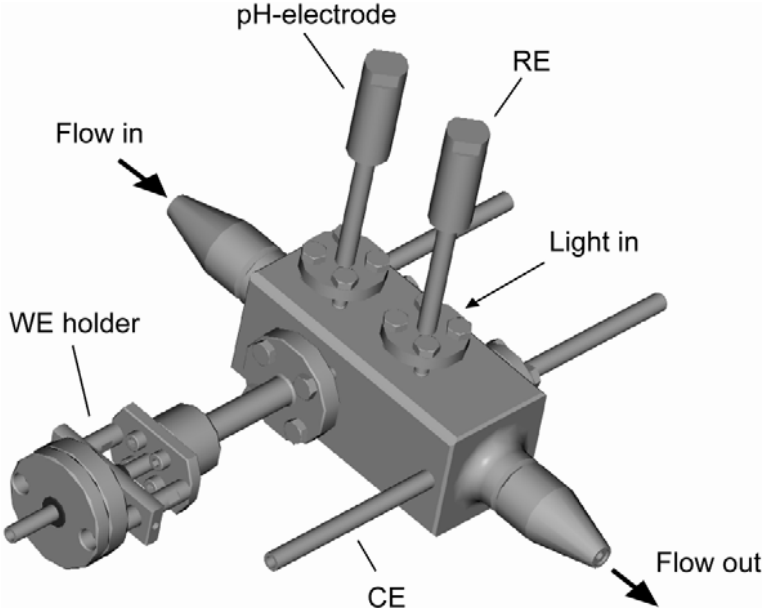

(a)

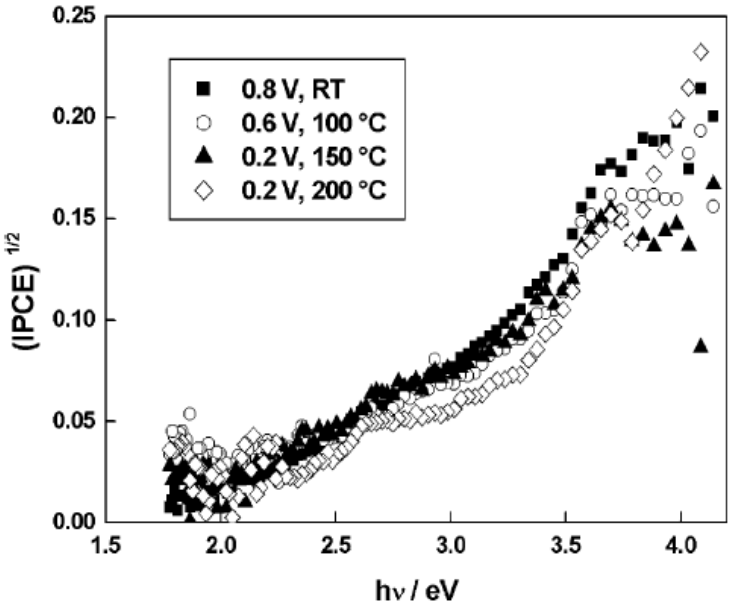

(b)

High temperature PEC III

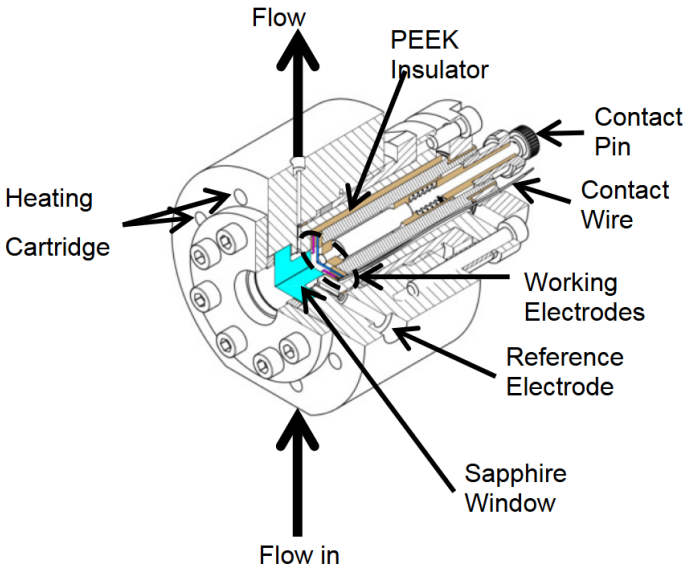

(a)

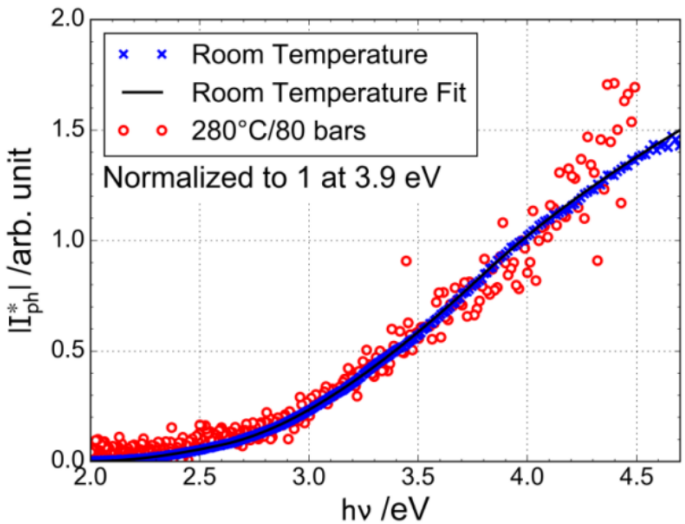

(b)

References I

[1] S. R. Morrison, *Electrochemistry at Semiconductor and Oxidized Metal Electrodes*. New York: Plenum Press, 1980.

[2] A. K. Vijh, "Correlation between bond energies and forbidden gaps of inorganic binary compounds," *Journal of Physics and Chemistry of Solids*, vol. 30, pp. 1999–2005, 1969.

[3] U. Stimming, "Photoelectrochemical studies of passive films," *Electrochimica Acta*, vol. 31, no. 4, pp. 415–429, 1986.

[4] F. Di Quarto, C. Sunseri, S. Piazza, and C. Sunseri, "Semiempirical Correlation between Optical Band Gap Values of Oxides and the Difference of Electronegativity of the Elements. Its Importance for a Quantitative Use of Photocurrent Spectroscopy in Corrosion Studies," *Journal of Physical Chemistry*, vol. 101, pp. 2519–2525, 1997.

[5] Y. Wouters, A. Galerie, and J.-P. Petit, "Photoelectrochemical Study of Oxides Thermally Grown on Titanium in Oxygen or Water Vapor Atmospheres," *Journal of The Electrochemical Society*, vol. 154, no. 10, pp. C587–C592, 2007.

[6] W. W. Gärtner, "Depletion-Layer Photoeffects in Semiconductors," *Physical Review*, vol. 116, no. 1, pp. 84–87, 1959.

[7] M. Butler, "Photoelectrolysis and physical properties of the semiconducting electrode WO_3," *Journal of Applied Physics*, vol. 48, no. 5, p. 1914, 1977.

[8] R. Benaboud, P. Bouvier, J.-P. Petit, Y. Wouters, and A. Galerie, "Comparative study and imaging by PhotoElectroChemical techniques of oxide films thermally grown on zirconium and Zircaloy-4," *Journal of Nuclear Materials*, vol. 360, no. 2, pp. 151–158, 2007.

[9] A. Srisrual, J.-P. Petit, Y. Wouters, C. Pascal, and A. Galerie, "Photoelectrochemical investigations on individual ferritic and austenitic grains of a duplex stainless steel oxidized in water vapour.," *Materials at High Temperatures*, vol. 28, no. 4, pp. 349–354, 2011.

[10] M. Bojinov, P. Kinnunen, T. Laitinen, K. Mäkelä, T. Saario, and P. Sirkiä, "Photocurrent response of the passive film on iron in a high-temperature aqueous electrolyte," *Electrochemistry Communications*, vol. 4, pp. 222–226, 2002.

[11] M. Skocic, "Etude (photo)-électrochimique en réacteur simulé du phénomène de shadow corrosion des alliages de zirconium," Ph.D. dissertation, Université de Grenoble Alpes, Grenoble, May 2016.

[12] A. Loucif, J.-P. Petit, and Y. Wouters, "Semiconducting behavior and bandgap energies of oxide films grown on alloy 600 under PWR simulated primary water conditions with different dissolved hydrogen contents," *Journal of Nuclear Materials*, vol. 443, no. 1–3, pp. 222–229, 2013.

References II

[13] A. J. Bard and M. Stratmann, *Fundamentals of Semiconductors Electrochemistry and Photoelectrochemistry*. Wiley-VCH, 2002.

[14] E. Becquerel, "Mémoire sur les effets électriques produits sous l'influence des rayons solaires," *Comptes Rendus des Séances Hebdomadaires*, vol. 9, pp. 561–567, 1839.

[15] A. W. Copeland, O. D. Black, and A. B. Garrett, "The Photovoltaic Effect," *Chemical Reviews*, vol. 31, no. 1, pp. 177–226, 1942.

[16] H. Finklea, "Photoelectrochemistry: Introductory concepts," *Journal of Chemical Education*, vol. 60, no. 4, p. 325, 1983.

[17] H. Gerischer, "Electrochemical Behavior of Semiconductors under Illumination," *Journal of The Electrochemical Society*, vol. 113, no. 11, pp. 1174–1182, 1966.

[18] H. Gerischer, "Semiconductor electrodes and their interaction with light," in *Photoelectrochemistry, Photocatalysis and Photoreactor*, M. Schiavello, Ed., Dordrecht: D. Reidel Publishing Company, 1985, pp. 39–106.

[19] P. Marcus and F. Mansfield, *Analytical Methods in Corrosion Science and Engineering*. Boca Raton, FL: CRC Press, 2006.

[20] J.-F. Marucco, *Chimie Des Solides*. Paris: EDP Sciences, 2006.

[21] R. Memming, *Semiconductor Electrochemistry*. Weinheim: WILEY-VCH Verlag GmbH, 2008.

[22] N. Sato, *Electrochemistry at Metal and Semiconductors Electrodes*. Amsterdam: Elsevier Science, 1998.

[23] W. Plieth, *Electrochemistry for Materials Science*. Amsterdam: Elsevier, 2008.

[24] P. R. Bevington and D. K. Robinson, *Data Reduction and Error Analysis for Physical Sciences*, Third. New York: McGraw Hill, 2003.

[25] J. D. Hunter, "Matplotlib: A 2D graphics environment," *Computing In Science and Engineering*, vol. 9, no. 3, pp. 90–95, 2007.

[26] E. Jones, T. Oliphant, P. Peterson, et al., *SciPy: Open source scientific tools for Python*, http://www.scipy.org/, 2020.

[27] J. Kiusalaas, *Numerical Methods in Engineering with Python*, Second. Cambridge: Cambridge University Press, 2010.

[28] H.-P. Langtangen, *A Primer on Scientific Programming with Python*, Third. Berlin Heidelberg: Springer, 2012.

References III

[29] K. J. Millman and M. Aivazis, "Python for Scientists and Engineers," *Computing in Science & Engineering*, vol. 13, no. 2, pp. 9–12, 2011.

[30] J. Nocedal and S. J. Wright, *Numerical Optimization*, Second. New York: Springer, 2006.

[31] T. E. Oliphant, "Python for Scientific Computing," *Computing in Science & Engineering*, vol. 9, no. 3, pp. 10–20, 2007.

[32] J.-P. Petit, R. Boichot, A. Loucif, A. Srisrual, and Y. Wouters, "Photoelectrochemistry of Oxidation Layers: A Novel Approach to Analyze Photocurrent Energy Spectra," *Oxidation of Metals*, vol. 1, pp. 1–11, 2013.

[33] W. H. Press, S. A. Teukolsky, W. T. Vetterling, and B. P. Flannery, *Numerical Recipes: The Art of Scientific Computing*, Third. Cambridge: Cambridge University Press, 2007.

[34] A. Srisrual, "Caractérisation photoélectrochimique d'oxydes thermiques développés sur métaux et alliages modèles," Thèse de Doctorat, Université de Grenoble, 2013.

[35] S. Van der Walt, S. C. Colbert, and G. Varoquaux, "The NumPy Array: A Structure for Efficient Numerical Computation," *Computing in Science & Engineering*, vol. 13, no. 2, pp. 22–30, 2011.